

# Changes in the content of eolian iron during the past 900 ka and the implications

WEI Jianjing<sup>1</sup> & GUO Zhengtang<sup>2,1</sup>

1. Institute of Geology and Geophysics, Chinese Academy of Sciences, Beijing 100029, China;

2. State Key Laboratory of Loess and Quaternary Geology, Institute of Earth Environment, Chinese Academy of Sciences, Xi'an 710075, China

Correspondence should be addressed to Guo Zhengtang (e-mail: ztguo@95777.com)

**Abstract** In this study, total Fe<sub>2</sub>O<sub>3</sub> content (Fe<sub>t</sub>) in two parallel sections from the central Loess Plateau (Xifeng and Changwu) is analyzed to address the variations of eolian iron in the past 900 ka. The obtained timeseries indicate that Fe<sub>t</sub> values in some glacial intervals are comparable to that of interglacial periods and its oscillations do not generally correspond to the long-term glacial-interglacial changes. Rather, it exhibits higher frequency fluctuations without detectable 100 ka period, but with a strong 20 ka period and a clear 40 ka period. The combination of 20 ka and 40 ka periods suggest that eolian iron content was relatively independent of glacial-interglacial changes, but more strongly influenced by the insolation changes in the northern hemisphere. Higher iron content was observed for the S5-1 soil that is correlative to marine δ<sup>18</sup>O stage 13. In marine records, this stage is characterized by higher δ<sup>13</sup>C values, suggesting that the event is of global significance.

**Keywords:** loess-paleosol sequences, eolian iron, paleoclimate, spectral analysis.

DOI: 10.1360/03wd0184

During the Quaternary, thick loess has been deposited at the middle reaches of the Yellow River in northern China within an area referred to as Loess Plateau<sup>[1]</sup>. Complete loess-soil sequences of the last 2.6 Ma are mostly more than 150 m in thickness, which are generally considered a near continuous paleoclimate record, containing more than fifty soil-forming intervals intercalated with dust deposition intervals<sup>[2]</sup>. Major interglacial soils and glacial loess units of the last 900 ka are labeled S0, L1, S1, L2, S2, ..., S8, L9 from the top to the bottom (Figs. 1 and 2) according to the Luochuan type section<sup>[1]</sup>. Eolian dust deposition and pedogenesis are, indeed, competing processes at all time, and the presence of a paleosol simply indicates that the latter process was predominant<sup>[3,4]</sup>. Stratigraphy of the loess-soil sequence is well correlative with that of the marine δ<sup>18</sup>O record<sup>[1]</sup>. The correlation pattern for the last 900 ka has now been commonly accepted<sup>[1,5]</sup> and that for the last 500 ka was also confirmed by an eolian record in the North Pacific<sup>[6]</sup>, a direct link

between the China loess and marine δ<sup>18</sup>O stratigraphy.

Eolian iron is thought to have significant effect on the ocean phytoplankton productivity, and thus may have played an important role in modulating global climates through influencing the CO<sub>2</sub> uptake of the ocean<sup>[7]</sup>. Eolian dust deposited in the Loess Plateau region is mainly originated from the desert lands in the Asian inland<sup>[1,3]</sup>. Meanwhile, a significant proportion from the same sources was transported by the westerly winds and deposited into the North Pacific region<sup>[6]</sup>. The temporal features of eolian iron as recorded in the loess-soil sequences in China would be helpful to understanding the eolian iron changes in the Pacific region.

This paper attempts to analyze the variations of eolian iron content in the past 900 ka based on two loess sections, one from Xifeng and another from Changwu, to investigate the spectral features of eolian iron changes, and to interpret the potential factors that influence eolian iron changes.

## 1 Materials and methods

The two studied Xifeng and Changwu loess sections are located at the central Loess Plateau, and thus may be more representative for characterizing the general situation of Quaternary loess deposits in northern China. Their stratigraphy correlates well with the other type loess sections<sup>[8]</sup>, such as Luochuan<sup>[1]</sup>. Magnetic susceptibility has been proven particularly useful for characterizing the stratigraphic boundaries of the loess-soil sequences in China<sup>[1,5]</sup> and the values are higher in soils than in the surrounding loess. In this study, 852 samples from Xifeng and 846 samples from Changwu were taken at 10 cm intervals. Susceptibility was measured on dry samples using a Bartington susceptibility meter. The timescales are obtained by correlation with the susceptibility curve of Kukla et al.<sup>[8]</sup> from the same site after a revision using the new paleomagnetic chronology. The last is dated by a magnetic susceptibility model<sup>[8]</sup> using the magnetic reversal boundaries as age controls. Although this model is based on some assumptions still contentious in part<sup>[9-11]</sup>, the yielded results are generally consistent with those obtained by land-sea correlation<sup>[5,6]</sup>, and thereby remains a working model for obtaining an independent timescale.

Total iron content of all samples taken from Xifeng and Changwu was analyzed and expressed as Fe<sub>2</sub>O<sub>3</sub> weight percentage (Fe<sub>t</sub>). The samples were dissolved by acid dissolving methods and the iron content was measured using a WFD-Y2 atomic adsorption unit with an analytical precision of 0.4%. The content of CaCO<sub>3</sub>, generally more or less translocated due to the pedogenesis, was gasvolumetrically measured on the same samples for rectified its dilution effect on iron concentration. The rectified values therefore represent those of the non-calcareous material. Microscopic thin sections of undisturbed soil and loess samples were fabricated to

evaluate the possibility of iron translocation during the formation of the soils. Spectral analyses of the magnetic susceptibility and  $Fe_{tr}$  time series were performed using the Maximum Entropy method.

## 2 Results and discussions

Figs. 1 and 2 show the variations of total  $Fe_2O_3$  ( $Fe_t$ )

in the two studied sections. They are compared with the magnetic susceptibility curves as a marker of stratigraphy (Figs. 1 and 2). As the formation of paleosols in the studied sections is characterized by significant dissolution and re-precipitation of  $CaCO_3$ , which affects the relative concentration of iron oxides-hydroxides,  $Fe_t$  values rectified

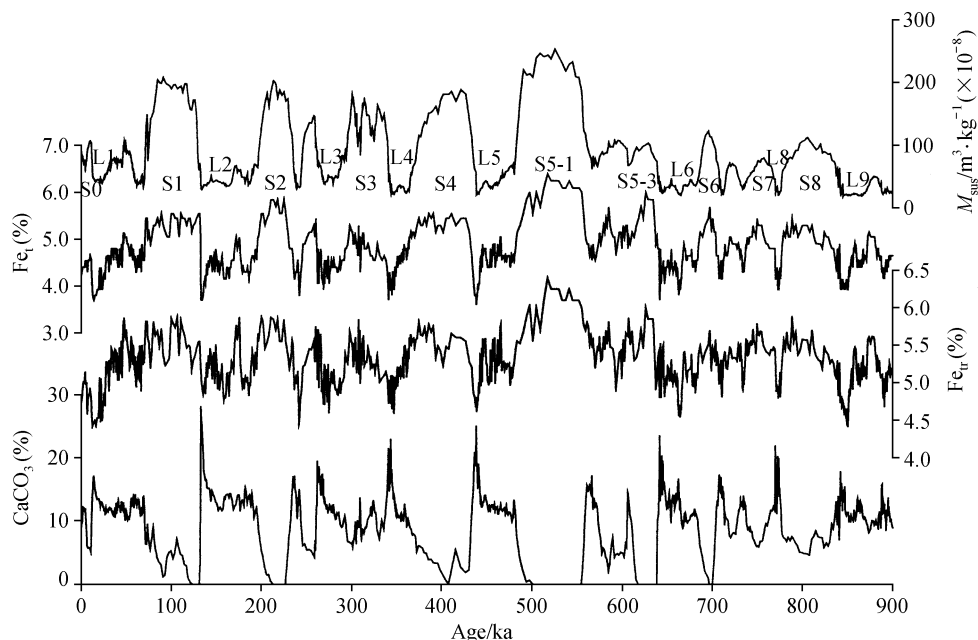


Fig. 1. Variations of magnetic susceptibility ( $M_{sus}$ ), total iron content ( $Fe_t$ ), total iron content rectified using  $CaCO_3$  content ( $Fe_{tr}$ ), and  $CaCO_3$  content in the Xifeng loess section.

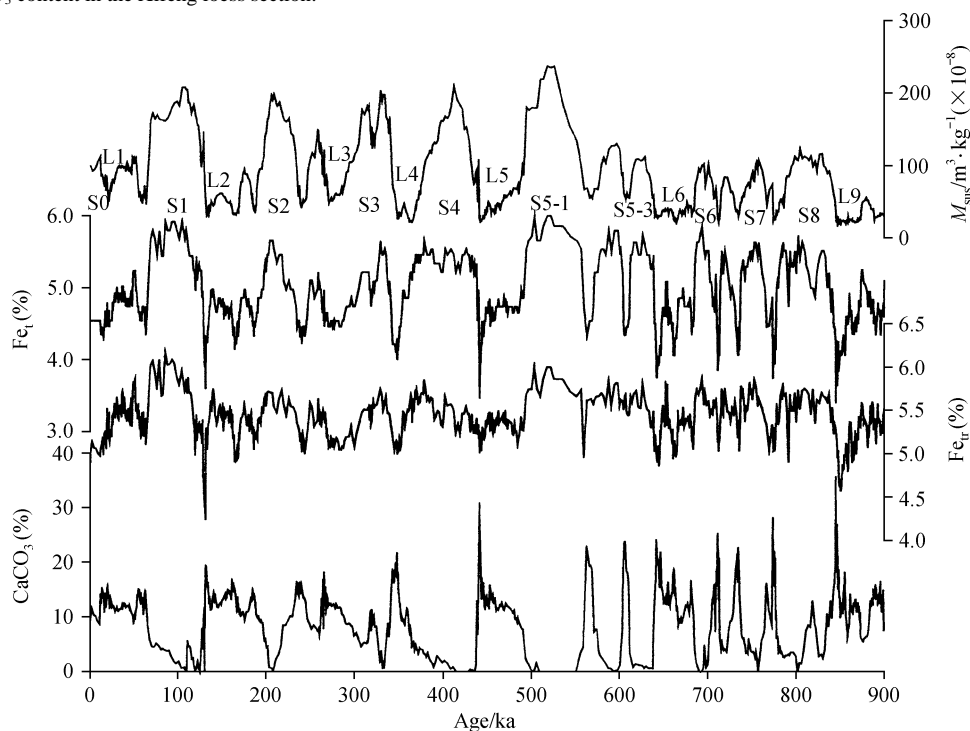


Fig. 2. Variations of magnetic susceptibility ( $M_{sus}$ ), total iron content ( $Fe_t$ ), total iron content rectified using  $CaCO_3$  content ( $Fe_{tr}$ ), and  $CaCO_3$  content in the Changwu loess section.

with the  $\text{CaCO}_3$  content ( $\text{Fe}_{\text{tr}}$ ) are given in Figs. 1 and 2.

Microscopic observations revealed only a small amount of clay coatings in the paleosols S1, S4, S5-1 and S5-3, the most strongly developed soils at the studied sites, and clay coating is absent in the other paleosols. Significant iron translocation related to clay illuviation process can therefore be basically ruled out. The lack of Fe-Mn hydromorphic features also precludes the possibility of significant iron redistribution in soluble state and exchange with the overlying and underlying loess. The  $\text{Fe}_{\text{tr}}$  values in the studied sections thereby mainly reflect the iron contents of eolian dust.

Variations of magnetic susceptibility in the sections clearly show the stratigraphy (Figs. 1 and 2).  $\text{CaCO}_3$  content is much lower in soil units than in loess, indicating strong decalcification of the soils. The non-rectified  $\text{Fe}_{\text{tr}}$  values are generally higher in soils than in loess, showing a higher consistency with magnetic susceptibility than for the rectified values ( $\text{Fe}_{\text{tr}}$ ). This is attributable to the dilution effect of  $\text{CaCO}_3$ , higher in loess than in soil units.

Since soluble salts other than  $\text{CaCO}_3$  in the central Loess Plateau are in a negligible amount, their effects to the iron content can be basically ruled out.

Figs. 1 and 2 show that  $\text{Fe}_{\text{tr}}$  did change through time. Its fluctuations do not generally correspond to the changes of magnetic susceptibility; rather they exhibit much higher frequency oscillations. Its values in some parts of the loess units are similar to those in soil units. Higher values are observed for S5-1 soil, which correspond to marine  $\delta^{18}\text{O}$  stages 13<sup>[1,5]</sup>. This soil represents a period of warm extreme of the last 2.6 Ma<sup>[12]</sup>. In marine records, this interval is characterized by higher  $\delta^{13}\text{C}$  values<sup>[13]</sup>, suggesting that it is of global significance.

In order to determine the temporal features of eolian iron fluctuations, spectral analyses were performed on both magnetic susceptibility and  $\text{Fe}_{\text{tr}}$ , using Maximum Entropy method<sup>[14]</sup> (Fig. 3). Magnetic susceptibility is usually used as a proxy of the East-Asian summer monsoon<sup>[3]</sup>, and therefore reflects climate changes in the Loess Plateau region. Magnetic susceptibility correlates well

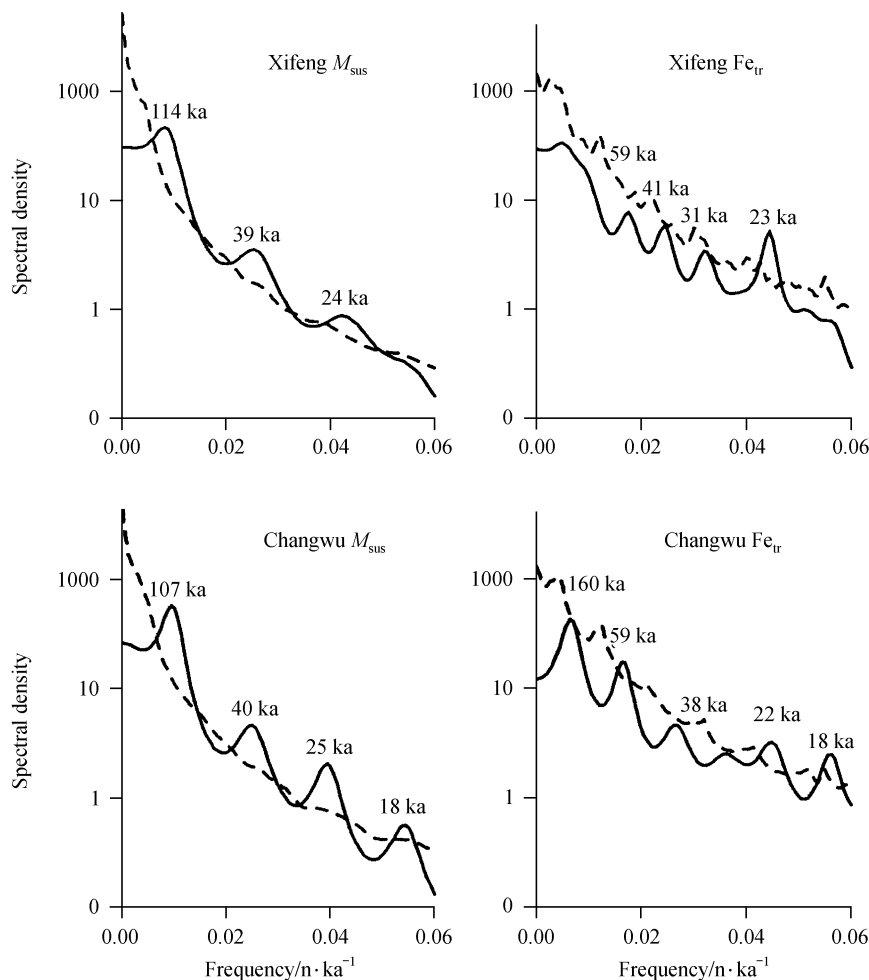


Fig. 3. Maximum Entropy spectral analyses of magnetic susceptibility ( $M_{\text{sus}}$ ) and eolian iron ( $\text{Fe}_{\text{tr}}$ ) time series. Continuous line represents the spectral density and dotted line represents the 95% confidence limit.

with the marine  $\delta^{18}\text{O}$  record, an indicator of global ice-volume<sup>[15]</sup>.

Spectral analyses on the Xifeng magnetic susceptibility timeseries revealed three discrete periods, centered respectively at 114, 39 and 24 ka with the spectral density well over the 95% confidence limit. The spectrum for magnetic susceptibility of Changwu is characterized by four periods at 107, 40, 25 and 18 ka, with the spectral density over the 95% confidence limit. Within the accuracy of the used timescales, which are independent of any land-sea correlation or orbital tuning, the 114 ka and 107 ka periods are correlative with the 100 ka period of the orbital eccentricity<sup>[16]</sup> while the periods of 39–40, 24–25 and 18 ka are consistent with the 40 ka period of the obliquity, the 23 ka and 19 ka periods of the precession, respectively.

The spectra calculated for  $\text{Fe}_{\text{tr}}$  of the two sections are quite different from those of magnetic susceptibility. The Xifeng  $\text{Fe}_{\text{tr}}$  timeseries is characterized by clear 59, 41, 31 and 23 ka periods, with the spectral densities of the 41 and 23 ka peaks over the 95% confidence limit. The Changwu  $\text{Fe}_{\text{tr}}$  spectrum shows five peaks at 160, 59, 38, 22 and 18 ka. The spectral densities for the 59, 22 and 18 ka peaks are well over the 95% confidence limit (Fig. 3). A remarkable feature is that the eccentricity period, centered at 100 ka<sup>[16]</sup>, is undetectable in the  $\text{Fe}_{\text{tr}}$  spectra for both sections.

The 114, 107, 39–40, 24–25 and 18 ka periods in the spectra of magnetic susceptibility indicate strong orbital control on loess deposition and soil formation in northern China over the past 900 ka, as was reported in earlier studies<sup>[17]</sup>. Because of the negligible effect of the eccentricity in modulating the solar insolation budget<sup>[16]</sup>, the ~100 ka period in geological records is usually interpreted as the signal of global ice-volume variations<sup>[18]</sup>. The strong 114 and 107 ka periods of the magnetic timeseries indicates a strong impact of glacial-interglacial cycles on Asian climate.

The 160 ka period in the Changwu  $\text{Fe}_{\text{tr}}$  record is not readily explainable by the astronomical theory. Besides this peak, the spectrum of the  $\text{Fe}_{\text{tr}}$  record from Changwu is indeed similar to that from Xifeng. The period at 59 ka has also been reported in a record of paleomagnetic variations<sup>[19]</sup>. This peak is of particular interest, as it has been predicted in a calculated orbital solution<sup>[20]</sup>, resulting from a combined effect of obliquity and precession<sup>[20]</sup>. The rough 40 and 20 ka periods are attributable to the periods of obliquity and precession, respectively. The most interesting result of this study is the lack of ~100 ka period in the  $\text{Fe}_{\text{tr}}$  timeseries, indicating a relative dynamic independence between the eolian iron content and the global ice-volume variations as are reflected by marine  $\delta^{18}\text{O}$  records<sup>[15]</sup>. Rather, the strong 23 ka period and a clear 40 ka period recorded in the  $\text{Fe}_{\text{tr}}$  timeseries would suggest a strong control of solar insolation, and the strong

23 ka period trends to suggest an insolation-forced factor of low latitude origin.

The mechanisms through which eolian iron content is more strongly influenced by insolation, but is relatively independent of global ice-volume variations are not yet clear, and need additional studies. These features may be helpful to further understanding the processes relative to eolian deflation, transportation and deposition. In view of the strong ~20 ka period that suggests an insolation-forced factor of low latitude origin, the strength of the summer monsoon could be one of the potential factors influencing the eolian iron content. Two possibilities might be invoked to explain the possible effects of the summer monsoon on eolian iron. Firstly, higher low-latitude insolation values may lead to stronger monsoon circulation<sup>[22]</sup>, of which the front would penetrate more deeply into the desert lands in northern China. Consequently, dust sources would be significantly changed following the oscillations of the monsoon front, which may lead to dust composition changes. Secondly, changes of the monsoon front may lead to changes in the distance between the dust sources and the deposition site. This may also lead to changes in eolian grain-size, and consequently to dust composition changes, because chemical composition of loess varies in different grain-size fraction<sup>[23]</sup>. If these were the cases,  $\text{Fe}_{\text{tr}}$  in the loess-soil sequences would bear some signals of the strength of the summer monsoon.

### 3 Conclusions

Our study yields a high-resolution record of eolian iron changes in the past 900 ka based on two parallel loess-soil sequences in the Loess Plateau region. The results show that eolian iron content is not in good agreement with the long-term glacial-interglacial oscillations. Rather, it exhibits much higher frequency fluctuations dominated by a strong ~23 ka and clear 41 ka orbital periods while the ~100 ka glacial-interglacial period is undetectable. These would suggest that eolian iron content was strongly forced by insolation changes in the Northern Hemisphere. The strength of the summer monsoon that is strongly forced by insolation is one of the potential factors influencing the eolian iron content.

Since eolian iron is thought to have significant effect on the ocean phytoplankton productivity<sup>[7]</sup>, the results would also provide a basis for further understanding its possible effects. Higher iron contents were observed for the S5-1 soil corresponding to marine  $\delta^{18}\text{O}$  stage 13. This interval is characterized in marine records by higher  $\delta^{13}\text{C}$  values, suggesting a global significance of the climate event.

**Acknowledgements** This work was supported by the National Natural Science Foundation of China (Grant No. 40231001) and the Chinese Academy of Sciences (Grant No. KZCX2-118).

## References

1. Liu, T. S. et al., *Loess and the Environment*, Beijing: China Ocean Press, 1985, 1—251.
2. Guo, Z. T., Ding, Z. L., Liu, T. S., *Pedosedimentary events in loess of China and Quaternary climatic cycles*, *Chinese Science Bulletin*, 1996, 41: 1189—1193.
3. An, Z. S., Kukla, G., Porter, S. C. et al., *Magnetic susceptibility evidence of monsoon variation on the loess plateau of central China during the last 130,000 years*, *Quaternary Research*, 1991, 36: 29—36.
4. Guo, Z. T., Biscaye, P., Wei, L. Y. et al., *Summer monsoon variations over the last 1.2 Ma from the weathering of loess-soil sequences in China*, *Geophysical Research Letters*, 2000, 27(12): 1751—1754.
5. Kukla, G., *Loess stratigraphy in central China*, *Quaternary Science Review*, 1987, 6: 191—219.
6. Hovan, S. A., Rea, D. K., Pisias, N. G. et al., *A direct link between the China loess and marine  $\delta^{18}\text{O}$  records: aeolian flux to the north Pacific*, *Nature*, 1989, 340: 296—298.
7. Martin, J. H., *Glacial-interglacial  $\text{CO}_2$  change: the iron hypothesis*, *Paleoceanography*, 1985, 5: 1—13.
8. Kukla, G., An, Z. S., Melice, J. L. et al., *Magnetic susceptibility record of Chinese loess*, *Trans. Royal Society of Edinburgh: Earth Sciences*, 1990, 81: 263—288.
9. Heller, F., Shen, C. D., Beer, J. et al., *Quantitative estimates of pedogenic ferromagnetic mineral formation in Chinese loess and palaeoclimatic implications*, *Earth and Planetary Science Letters*, 1993, 114: 385—390.
10. Verosub, K. L., Fine, P., Singer, M. J. et al., *Pedogenesis and palaeoclimate: interpretation of the magnetic susceptibility record of Chinese loess-palaeosol sequences*, *Geology*, 1993, 21: 1011—1014.
11. Han, J. M., Lu, H. Y., Wu, N. Q. et al., *The magnetic susceptibility of modern soils in China and its use for palaeoclimatic reconstruction*, *Studia Geophysica and Geodaetica*, 1996, 40: 262—275.
12. Guo, Z. T., Liu, T. S., Fedoroff, N. et al., *Climate extremes in Loess of China coupled with the strength of deep-water formation in the North Atlantic*, *Global and Planetary Change*, 1998, 18: 113—128.
13. Raymo, M. E., Oppo, D. W., Curry, W., *The mid-Pleistocene climate transition: a deep sea carbon isotopic perspective*, *Paleoceanography*, 1997, 12: 546—559.
14. Burg, J. P., *Maximum entropy spectral analysis: Presented at the 37th Annual International SEG Meeting November 1*, in Oklahoma City, 1967.
15. Shackleton, N. J., Hall, M. A., *Oxygen and carbon isotope stratigraphy of deep sea drilling project Hole 552A: Plio-Pleistocene glacial history*, *Initial Reports of the Deep Sea Drilling Project*, 1984, 81: 599—609.
16. Berger, A., Loutre, M. F., *Insolation values for the climate of the last 10 million years*, *Quaternary Science Review*, 1991, 10: 297—317.
17. Ding, Z. L., Liu, T. S., Rutter, N. et al., *Ice-volume forcing of east Asian winter monsoon variations in the past 800000 years*, *Quaternary Research*, 1995, 44: 149—159.
18. Imbrie, J., Hays, J. D., Martinson, D. et al., *The orbital theory of Pleistocene climate: support from a revised chronology of marine  $\delta^{18}\text{O}$  record* (eds. Berger, A., Imbrie, J., Hays, J. et al.), *Milankovitch and Climate*, Part 1. Dordrecht, Netherlands: D. Reidel Publishing Co., 1984. 265—305.
19. Negi, J. G., Tiwari, R. K., *Periodicities of palaeomagnetic intensity and palaeoclimatic variations: a Walsh spectral approach*, *Earth and Planetary Science Letters*, 1984, 70: 139—147.
20. Berger, A. L., *Support for the astronomical theory of climatic change*, *Nature*, 1977, 269: 44—45.
21. Guo, Z. T., Petit-Maire, N., Kropelin, S., *Holocene non-orbital climatic events in present-day arid areas of northern Africa and China*, *Global and Planetary Change*, 2000, 26: 97—103.
22. Clemens, S., Prell, W., Murray, D. et al., *Forcing mechanisms of the Indian Ocean monsoon*, *Nature*, 1991, 353: 720—725.
23. Peng, S. Z., Guo, Z. T., *Geochemical indicator of original eolian grain size and the implications on winter monsoon evolution*, *Sci. Chin., Series D*, 44(Suppl.): 261—266.

(Received April 5, 2003; accepted May, 12, 2003)